

TeV J2032+4130: a not-so-dark Accelerator?

Y. M. Butt¹, J. A. Combi², J. Drake¹, J. P. Finley³, A. Konopelko³,
M. Lister³, J. Rodriguez⁴, D. Shepherd⁵

Abstract

The HEGRA gamma-ray source TeV J2032+4130 is considered the prototypical “dark accelerator”, since it was the first TeV source detected with no firm counterparts at lower frequencies. The Whipple collaboration has observed this source in 2003-5 and those data indicate that the Whipple TeV emission hotspot is displaced about 9 arcminutes to the northeast of the HEGRA position. Here we report on a dual-lobed non-thermal radio source that appears in the Westerbork Synthesis Radio Telescope (WSRT) dataset consistent with the locations of the Whipple and, to a lesser extent, also the HEGRA hotspot. A weak diffuse non-thermal radio condensation exists ~5 arcmin to the SW of this source, along the axis of the lobes and thus may be related. We also find a weak predominantly non-thermal shell-like supernova remnant (SNR)-type object, with a location and morphology very similar to the HEGRA source, in our VLA dataset at 4.8 GHz. Thus, either of these objects – or perhaps even both – may be viable counterparts of the reported very high energy (VHE) gamma-ray emissions in this region. If so, TeV J2032+4130 may not be a “dark accelerator” after all. Further observations with the new generation of imaging Cherenkov telescopes are needed to pin down the location and morphology of the TeV emission region and thus clear up the confusion over its possible lower frequency counterparts.

¹ *Harvard-Smithsonian Center for Astrophysics, 60 Garden St., Cambridge, MA 02138, USA*

² *Departamento de Física (EPS), Universidad de Jaén, Campus Las Lagunillas s/n, 23071 Jaén, SPAIN*

³ *Department of Physics, Purdue University, West Lafayette, IN 47907, USA*

⁴ *CEA Saclay, DSM/DAPNIA/SaP, F-91191 Gif sur Yvette, FRANCE*

⁵ *NRAO, P.O. Box O, Socorro, NM 87801-0387, USA*

Introduction

In 2002 the HEGRA collaboration reported on a steady and extended (~ 6.2 arcmin radius) TeV gamma-ray emitting region, TeV J2032+4130, near the massive stellar association Cygnus OB2 (Aharonian et al., 2002, 2005). We followed-up this source using the VLA and CHANDRA, but found no obvious counterparts at the lower frequencies (Butt et al., 2003, 2006; Mukherjee et al., 2003, 2006). Paredes et al. (2006) have recently reported on some deeper radio observations which do show a handful of very interesting potential counterparts. Several possible origins of the gamma-ray emission have been suggested in the literature having to do, variously, with the termination lobes of Cyg X-3 (Aharonian et al., 2002; see also, Marti, Paredes & Peracaula 2000); the stellar winds in Cyg OB2 (Aharonian et al., 2002; Butt et al., 2003; 2006; Domingo-Santamaria & Torres, 2006); a possible proton-blazar (Mukherjee et al., 2003); a pulsar wind nebula (Bednarek 2003; 2006); or possible microquasars (Paredes et al., 2006). However, since none of these possible scenarios has yet been conclusively verified, this, and other similar TeV sources without firm counterparts, have been dubbed “dark accelerators” by some authors. It is commonly believed that they are most likely of hadronic origin. TeV J2032+4130, being the first discovered is, in fact, the prototype of this informal class of sources.

Using archival 10m data from 1989-90, the Whipple collaboration confirmed the existence of TeV J2032+4130 (Lang et al., 2004), and more recently a total of 65.5 hr of Whipple data taken during 2003-2005 towards this source has been reported (Konopelko et al. 2006). The analysis of the latest dataset reveals a distinct excess in the field of view at a significance of 6σ . The centroid position of this γ -ray source is $\alpha=20^{\text{h}}32^{\text{m}}27^{\text{s}}$, $\delta=41^{\circ}39'17''$ and the estimated integral flux is about 8% of the Crab-Nebula flux. The data are consistent with a point-like source, even though an extended source with an effective radius less than $7'$ cannot be ruled out. The center of gravity of the γ -ray emission as seen in the Whipple data is about 9 arcmin northeast of that reported by HEGRA. However, given the statistical and systematic uncertainties in the source localization, which are $\sim 4'$ and $6'$, respectively, the Whipple hotspot location can be considered consistent with the HEGRA γ -ray source position [Fig. 1a].

Radio Analysis

We reanalyzed the WSRT data of Setia-Gunawan et al. (2003; hereafter SG2003) using standard procedures with the AIPS package of the National Radio Astronomy Observatory (NRAO). For

these observations the WSRT beam size at 1.4GHz and 350 MHz was $13'' \times 19''$ and $48'' \times 75''$ respectively. The limiting flux-densities were $\sim 2\text{mJy}$ at 1.4GHz and $\sim 7\text{mJy}$ at 350MHz. We convolved the radio map at 1420 MHz with a similar synthesized beam as the 350 MHz observations in order to perform the spectral index measurements.

We previously noted two non-thermal radio sources with a jet-like structure marginally coincident with the HEGRA position in the WSRT data reported by SG2003 at 350 MHz and 1.4 GHz (see Table 3 in Butt et al., 2006; hereafter B2006). We have independently recalculated the intensities and spectral indices of the dual-lobed radio structure and find that they agree with the values stated by SG2003 (Table 1).

# (SG2003)	Position (J2000)	1.4GHz Flux Density	350MHz Flux Density	Sp. Index
217	20 32 1.22, +41 37 13.64	$36 \pm 6 \text{ mJy}$	$87 \pm 6 \text{ mJy}$	-0.65
218	20 32 2.16, +41 37 59.24	$39 \pm 6 \text{ mJy}$	$122 \pm 3 \text{ mJy}$	-0.84

Table 1: Characteristics of the non-thermal dual-lobe radio object found in WSRT data.

There is also a weak diffuse non-thermal radio condensation roughly aligned with the axis of the lobes located ~ 5 arcmin further SW of the dual-lobed jet-like source, but it is unknown whether the structures are related (Fig. 2). This radio source is located at $\alpha_{2000}, \delta_{2000} \sim (20\ 31\ 53, +41\ 32\ 35)$ and has a 365MHz flux of $\sim 11.6\text{mJy}$. At 1400MHz, the source is so weak that it is only marginally above the noise level of $\sim 2\text{mJy}$. The spectral index of this radio emission is -1.3 ± 0.5 . Two other non-thermal radio sources also exist in the extended radio field, one of which is also dual-lobed. However, the locations of these sources are inconsistent with the position of either one or both TeV gamma-ray hotspots, and therefore we do not consider them likely counterparts of the TeV emission (Fig. 1a). To estimate the total diffuse radio flux in the extended radio emission region coincident with the Whipple hotspot, we considered all the radio flux with the elliptical region shown in Fig. 1, except for that due to the dual-lobed radio source. We found the following flux densities at the two frequencies for the diffuse radio emission in this region: $F(350 \text{ MHz}) = 2.1 \pm 0.3 \text{ Jy}$ and $F(1420 \text{ MHz}) = 2.8 \pm 0.4 \text{ Jy}$.

On April 29 2003 we had also carried out a mosaic observation of the TeV J2032+4130 source region with the VLA⁶. The array was in the D-configuration and the flux calibrator was 3C48 and

⁶ NRAO VLA proposal AB1075 (PI: Butt) Observed April 29, 2003. 10 hours total in a five-pointing exposure at 6 and 20cm. The NRAO is a facility of the NSF operated under cooperative agreement by Associated Universities, Inc.

the gain calibrator, J2007+404. The source fields were observed with 3.5 to 6' spacing in a 5-point pattern, the primary beam of the VLA at 4.85 GHz being about 9'.

The resulting 6cm data were reduced with the Common Astronomy Software Applications (CASA) software and imaged with Astronomical Information Processing Software (AIPS++). The final mosaic image was weighted with robust weighting that provided an optimal compromise between point source sensitivity and minimum noise levels. The image was gridded to form a single mosaic and then deconvolved with a CLEAN algorithm that allowed multiple scales to be used for the clean components to maximize sensitivity to extended structure while still preserving the image flux density. The resulting image (Fig. 3) has uniform sensitivity across the mosaic field, however the flux density decreases toward the edge of the field as the primary beam response decreased.

The flux was measured in an image that was corrected for the mosaic primary beam response so the flux density was constant while the noise increased toward the edge of the mosaic field. The extended structure has a flux density of approximately 225 mJy at 6cm. In comparing the 6cm data with the 20cm as analyzed by Paredes et al. (2006), it is evident that the western region of this extended shell-like structure is predominantly non-thermal. This structure is centered approximately at $\alpha_{2000}, \delta_{2000} = (20\ 31\ 55, +41\ 29\ 00)$ with a radius of about 5 arcmin, consistent with the reported location and extension of the HEGRA source. The emission is weak and at 1.4GHz only the western part of the full ring-like structure is evident. The radio spectral index is variable across the structure and ranges from $\alpha \sim -0.7$ in the west, to $\sim +0.6$ or larger in the east, as shown in Fig 3. We can thus tentatively say that the western region of this object is more non-thermal than the rest of the structure. This radio ring is not evident in the 365 MHz WSRT data but this may be due to that interferometer being optimized for higher-resolution at the expense of diffuse sensitivity.

Chandra

A Chandra X-ray Observatory ACIS-I observation of the region in the vicinity of TeV J2032+4131 was described by B2006. Here, we reanalyzed the same 48728s exposure. Analysis was performed using CIAO software Version 3.3.0.1. B2006 listed sources found by an automated wavelet-base source detection algorithm “*wavedetect*”, and three sources from that list that fall close to the radio source: 36 (**E** in Fig. 1), 153 (**F** in Fig.1) and 227 (**G** in Fig. 1; this is

the same as source 1 of Mukherjee et al., 2003). Of these, 36 and 153 are faint while 227 is a bright source with a count rate of about 0.015 count/s. In addition to these sources, we also located by eye two additional regions of enhanced X-ray brightness that appear to be slightly more extended than a point source due to the effects of point spread function (psf)-distortion this far off-axis. One of these falls between the two radio lobes but is off-set slightly east of their centre; the other is coincident with the southern radio lobe. These two regions of enhanced X-ray brightness can each be described by two positions derived from a 8× binned image of the field: Central (**A & B** in Fig. 1) , with $\alpha_{2000}, \delta_{2000} = (20\ 32\ 02.4, +41\ 37\ 37)$ and $\alpha_{2000}, \delta_{2000} = (20\ 32\ 02.1, +41\ 37\ 34)$; and the southern-lobe (**C & D** in Fig. 1), with $\alpha_{2000}, \delta_{2000} = (20\ 32\ 01, +41\ 37\ 10.6)$ and $\alpha_{2000}, \delta_{2000} = (20\ 32\ 00.6, +41\ 37\ 06.7)$. We find both that these regions are rather hard, containing more counts in the 2-10keV band than in the 0.5-2keV one.

The diffuse non-thermal radio condensation located ~5 arcmin SW of the dual-lobed source also has two X-ray sources coincident with its location: SW Condensation X1: $\alpha_{2000}, \delta_{2000} = (20\ 31\ 52.71, +41\ 32\ 40.20)$ and SW Condensation X2: $\alpha_{2000}, \delta_{2000} = (20\ 31\ 52.49, +41\ 32\ 09.43)$. The first is likely the X-ray counterpart of star #157 of Massey & Thompson (1991) at $\alpha_{2000}, \delta_{2000} = (20\ 31\ 52.63, +41\ 32\ 40.7)$, whereas the second could truly be a genuine X-ray counterpart of the radio condensation. The X-ray event characteristics of all these sources nearby or coincident with the relevant radio structures are listed in Table 2.

<i>X-ray Source</i>	Cts*	S/N	Frac. 0.5-2.5 keV	Frac. 2.5-10 keV	X-ray Flux (erg cm ² s ⁻¹)
Central: A&B	32	2.8	0.28	0.72	$\sim 1.8 \times 10^{-14}$
South-lobe: C&D	47	2.6	0.38	0.62	$\sim 2.6 \times 10^{-14}$
SW condensation X1	9	2.9	0.89	0.11	$\sim 5 \times 10^{-15}$
SW condensation X2	9	2.8	0.56	0.44	$\sim 5 \times 10^{-15}$
B2006:36 E	24	2.3	0.38	0.62	$\sim 1.3 \times 10^{-14}$
B2006:153 F	29	2.5	0.48	0.52	$\sim 1.6 \times 10^{-14}$
B2006:227 G	718	26.0	0.31	0.69	$\sim 4 \times 10^{-13}$
Background	-	-	0.29	0.71	-

Table 2: Characteristics of Chandra sources detected nearby or coincident with the non-thermal dual-lobe radio object. Note that the lobe sources are both rather hard in X-rays.

* *total counts in source region (ie source + background)*

Infrared, Optical and Hard X-ray Bands

At the very center of the dual-lobed radio structure, coincident with the X-ray emission of sources **A** & **B**, lies a 2MASS infrared source, 2MASS 20320186+4137377, with standard magnitudes $J=16.401\pm0.107$, $H=15.325\pm0.096$ and $K=14.879$. With the present available information, however, it is impossible to tell if this object is stellar or not, since a spectrum is not available. There are also several other 2MASS sources nearby or coincident with the radio lobes, as shown in Fig 1b, but it is unclear if these are related to this source.

We inspected the USNO-B1.0 catalog (Monet et al., 2003), but found no objects coincident with the central 2MASS source at optical wavelengths. However there is a star at: $\alpha_{2000}, \delta_{2000} = (20\ 32\ 00.1, +41\ 37\ 14)$ with $B_{\text{mag}}=15.46$, $V_{\text{mag}}=14.00$ (Star #179 in Massey & Thompson 1991), marginally coincident with the southern lobe of the radio structure. This star is also designated GSC 03161-00887.

We also reduced INTEGRAL/IBIS hard X-ray data with the Off line Scientific Analysis (OSA) software package version 6.0. We focused on the data from the IBIS Soft Gamma-ray Imager (ISGRI, Lebrun et al. 2003) which has the highest sensitivity and best angular resolution up to ~ 200 keV. We extracted images in four energy ranges, namely 20-40 keV, 40-80 keV, 80-150 keV and 150-300 keV, from all public science windows (scw, i.e. INTEGRAL pointings) that were less than 15 degrees from the Galactic Black hole Cyg X-1. This resulted in 1565 good scw between revolutions 12 and 218, for a total exposure time of about 3 Ms. None of the very high energy sources was spontaneously detected by the software. The presence of bright sources as Cyg X-1 and Cyg X-3 in the field can be a cause of artifacts (fake sources) in mosaics of such a long accumulation time. We thus verified that the TeV J2032+4130 location did not fall on any such artifact. We estimated 3σ upper limits from the values of the variance at the gamma-ray position and the efficiency of the source detection in each energy range, following $\text{Upper Limit} = 3 \text{ var}^{1/2} / \text{Efficiency}$. We found no positive detection of TeV J2032+4130 in the 20-300keV band and derived the following 3σ upper limits: 20-40 keV : 0.40 mCrab; 40-80 keV : 0.85 mCrab; 80-150 keV: 2.2 mCrab; 150-300 keV: 50 mCrab.

Discussion & Conclusions

Motivated by the more northerly location of the center-of-gravity of Whipple hotspots (Lang et al. 2004; Konopelko et al., 2006) for the source TeV J2032+4130, as compared with the HEGRA one (Aharonian et al., 2002; 2005) we undertook a multiwavelength study of that region in pursuit of possible lower frequency counterparts of the high-energy emission observed.

We find a dual-lobed non-thermal radio object consistent with the position of the Whipple hotspot, and to a lesser extent, also the HEGRA TeV emission region. There is a 2MASS infrared source (2MASS 20320186+4137377) and coincident X-ray emission (sources **A** & **B**) at the center of this radio structure. The latter could be a signature of X-ray emission from nearby the putative compact object or disk emission. At least the southern radio lobe also appears to emit in X-rays, and quite possibly the northern one also. Both the central and southern lobe X-ray sources appear to have a hard spectrum, such as may be expected from an absorbed source, but the statistics are poor (Table 2). The X-ray emission from the lobe(s) might be the result of fast shocks that travel along the radio jet, heating the gas up to very high temperatures. There is also a weak diffuse non-thermal radio source roughly aligned with the axis of the lobes and located about 5 arcmin SW [$\alpha_{2000}, \delta_{2000} = (20\ 31\ 53, +41\ 32\ 35)$ with a 365MHz flux of ~ 11.6 mJy, see Fig. 2], but it is unknown whether the structures are related. This source is notable since it is located within the HEGRA emission region, and is also diffuse. If this source is a TeV emitter, in addition to the suggested dual-lobed jet-like object, then it is possible that the extension reported by HEGRA (and not ruled out by Whipple) arises from the composite nature of these two emission regions.

With the information available we cannot yet make a definitive statement on the nature of the dual-lobed jet-like non-thermal radio source. If Galactic, it could well be a microquasar (eg. Bosch-Ramon, Aharonian and Paredes, 2005; Paredes 2006) or, less likely, pulsar-related (eg. Bednarek, 2006); if extragalactic, it is most likely a radiogalaxy with powerful dual radio cocoons. M87 and Centaurus A are examples of TeV- and GeV-emitting non-blazar radiogalaxies, respectively (eg. Grindlay et al., 1975; Sreekumar et al., 1999; Beilicke et al., 2005; Combi et al., 2003); however, at least in the case of M87, the VHE emission appears to be point-like and rapidly variable (Aharonian et al., 2006). On longer, year-long, timescales, however, M87 appears to be much more steady. To better discriminate between the Galactic vs. extragalactic alternative one would need to detect the central object at optical and/or IR

frequencies and obtain a spectrum to be able to test for the possible redshift of the H-alpha or other emission lines. If no redshift is found it would of course imply that this source is Galactic, possibly similar to a number of highly-absorbed INTEGRAL sources recently discovered (eg. Filliatre & Chaty, 2004; Chaty & Rahoui, 2006). Interestingly, even if this radio source is unrelated to the gamma-ray emission reported by Whipple and HEGRA, it would still make an excellent candidate counterpart of the strong flaring TeV emission reported by the Crimean Astrophysical Observatory approximately 0.7° North of Cygnus X-3 (Neshpor et al., 1995).

Besides the dual-lobed source, relatively strong extended radio emission is also present within the area of the Whipple hotspot. Though this could also conceivably be a radio counterpart of the TeV emission, this extended radio emission is thermal in nature, with a mean index of $+0.12 \pm 0.1$. Furthermore, the extended thermal radio region lies well outside the HEGRA TeV J2032+4130 location. For these two reasons we disfavor its direct association with TeV J2032+4130.

We have discussed above the possible association of the dual-lobed radio structure, together with its plausibly related radio condensation 5 arcmin to the SW, with TeV J2032+4130. However, we emphasize that the case is far from closed. The alternate associations of this VHE source with possible microquasars (Paredes et al., 2006) or with an outlying sub-group of very massive and powerful stars in Cyg OB2 are also somewhat persuasive (see, eg., Fig 1 in Butt et al., 2003 and Fig. 3 in B2006). In fact, Anchordoqui et al. (2006a, 2006b) have recently proposed an interesting new hypothesis for the origin of the high energy flux in the latter scenario: they suggest that the TeV gamma-rays could result from the photo-deexcitation of PeV energy nuclei that are themselves the photo-disintegration products of heavier nuclei broken-up in a bath of intense ultraviolet photons, such as would be present in Cyg OB2. Other interesting phenomena, such as possible time-correlated supernovae of a previous generation of stars in the Cyg OB2 region – which may have led to the ejection of sets of binary pulsars (Vlemmings, Cordes and Chatterjee 2004) – may also be involved in untangling the true scenario of the origin of the TeV flux seen here.

VLA data at 4.8 GHz also hints at the presence of a weak (~ 225 mJy at 4.8GHz) SNR-like object with a radius of about 5 arcmin which is consistent with the 1σ extension reported by HEGRA for TeV J2032+4130 (Fig. 3). The center of this ring-like structure is approximately $\alpha_{2000}, \delta_{2000} = (20\ 31\ 55, +41\ 29\ 00)$, also consistent with the HEGRA report and at least its western part is non-thermal. Assuming this object is an SNR co-located with Cyg OB2, at a distance of 1.7 kpc, its

radius would be only ~ 3 pc and its age as low as ~ 500 years. Note that the SNR G347.5-0.6 also is TeV bright and radio-dim. Alternatively, this radio ring may also be due to multiple large-scale shocks created by several of the very powerful stars in Cyg OB2 (eg., Cesarsky & Montmerle, 1983). It remains to be seen whether this intriguing, dominantly non-thermal, radio object may be related to the VHE gamma-ray emission. Deeper, more sensitive observations of this region at a handful of radio frequencies would be very useful to extract higher-fidelity data on this interesting structure.

A proper understanding of TeV J2032+4130 may also need to take into account the recent results from the air-shower arrays MILAGRO and TIBET, which have shown the entire Cygnus region to be a bright source of TeV gamma-rays (Atkins et al., 2005) and possibly also cosmic rays (Amenomori et al., 2006; Abdo et al., 2006). Clearly it would be very helpful to better determine the true location and morphology of the TeV gamma-ray emission region (TeV J2032+4130) with higher precision. This is something that the new generation of Imaging Cherenkov telescopes are ideally suited for doing. We estimate, for instance, that just 20 hrs of VERITAS time could yield a 6 sigma detection which would allow one to properly localize this source, and, simultaneously, give better morphological information possibly confirming or denying its association with the various possible lower frequency counterparts in the region.

References

- Abdo, A., et al., 2006, ApJ Lett. submitted, astro-ph/0611691
- Aharonian, F., et al. 2002, A&A, 393, L37
- Aharonian, F. et al., 2005, A&A, 431, 197
- Aharonian, F., et al., 2006, Science, Vol. 314. no. 5804, pp. 1424 - 1427
- Anchordoqui, L. et al., 2006a, astro-ph/0611580
- Anchordoqui, L. et al., 2006b, astro-ph/0611581
- Amenomori, M., et al., 2006, Science, 314, 439 astro-ph/0610671
- Atkins, R., et al., 2005, Phys Rev Lett. 95, 1103
- Bednarek, W., 2003, MNRAS, 345, 847
- Bednarek, W., 2006, astro-ph/0610307, Proc. Multimessenger approach to high energy gamma-ray sources, 2006.

Beilicke, M, et al., in Proc. 29th ICRC. August 3-10, 2005, Pune, India. Volume 4, p.299.
 Available on-line: <http://icrc2005.tifr.res.in/htm/Vol-Web/Vol-14/14299-ger-beilicke-M-abs1-og23-oral.pdf>

Bosch-Ramon, V., Aharonian, F., and Paredes, J. M., 2005, "Astrophysical Sources Of High Energy Particles and Radiation", June 2005, AIP Conf. Proc., Vol. 801, 196, astro-ph/0605489

Butt, Y., et al. 2003, ApJ, 597, 494

Butt, Y., et al., 2006, ApJ, 643, 238

Cesarsky, C. J. and Montmerle, T., 1983, Space Science Reviews, vol. 36, Oct. 1983, p. 173-193.

Chaty, S., & Rahoui, F., in Proc. 6th INTEGRAL Workshop, The Obscured Universe, Space Research Institute, Moscow, Russia, July 2-8, 2006, astro-ph/0609474

Combi, J. A., et al., 2003, ApJ 588, 731

Dickey & Lockman, 1990, Annu. Rev. Astron. Astrophys., 28, 215

Domingo-Santamaria, E., & Torres, D., 2006, A&A 448, 613

Filliatre, P., & Chaty, S., 2004, ApJ, 616, 469

Georganopoulos, M., Perlman, E. & Kazanas, D., 2005 ApJL 634, 33

Grindlay, J., et al., 1975, ApJL 197, L9

Konopelko, A., et al. (VERITAS collaboration), 2006, ApJ, accepted – available on astro-ph

Lang, M.J., et al. 2004, A&A, 423, 415

Lebrun, F., et al., 2003, A&A, 411L, 141

Massey, P. & Thompson, A. B., 1991, Astron. J., 101, 1408

Monet, D. G., et al., 2003, AJ, 125, 984

Mukherjee, R., et al., 2003, ApJ, 589, 487

Mukherjee, R., et al., 2006, in "The Multi-Messenger Approach to High-Energy Gamma-ray Sources" Proc., Barcelona/Spain (2006), astro-ph/0610299

Neshpor, Y.I., et al., 1995, Proc. 24th ICRC (Rome), 2, 385

Paredes, J. M., 2006, Proc. Vulcano Workshop 2006 "Frontier Objects in Astrophysics and Particle Physics", Bologna, Italy, astro-ph/0609168

Paredes, J. M., et al., 2006 ApJL accepted, astro-ph/0611881

Setia Gunawan, D. Y. A., et al., Ap J SS, 149, 123, 2003

Sreekumar, P., et al., 1999 Astroparticle Physics 11, 221

Taylor, A. R., et al., 1996 ApJS, 107, 239

Vlemmings, W. H. T., Cordes, J. M. and Chatterjee, S., 2004, ApJ 610, 402

Wendker, H. J., Higgs, L. A., and Landecker, T. L., 1991, A&A, 241, 551

Acknowledgements

YMB is supported by NASA/Chandra and NASA/INTEGRAL GO Grants and a NASA LTSA Grant. JPF and AK thank the US DOE for their continued support. JAC is a researcher of the program Ramon y Cajal funded jointly by the Spanish Ministerio de Ciencia y Tecnologia and Universidad de Jaen. J. C. also acknowledges support by DGI of the Spanish Ministerio de Educacion y Ciencia under grants AYA2004-07171-C02-02 and FEDER funds and Plan Andaluz de Investigacion of Junta de Andalucia as research group FQM322.

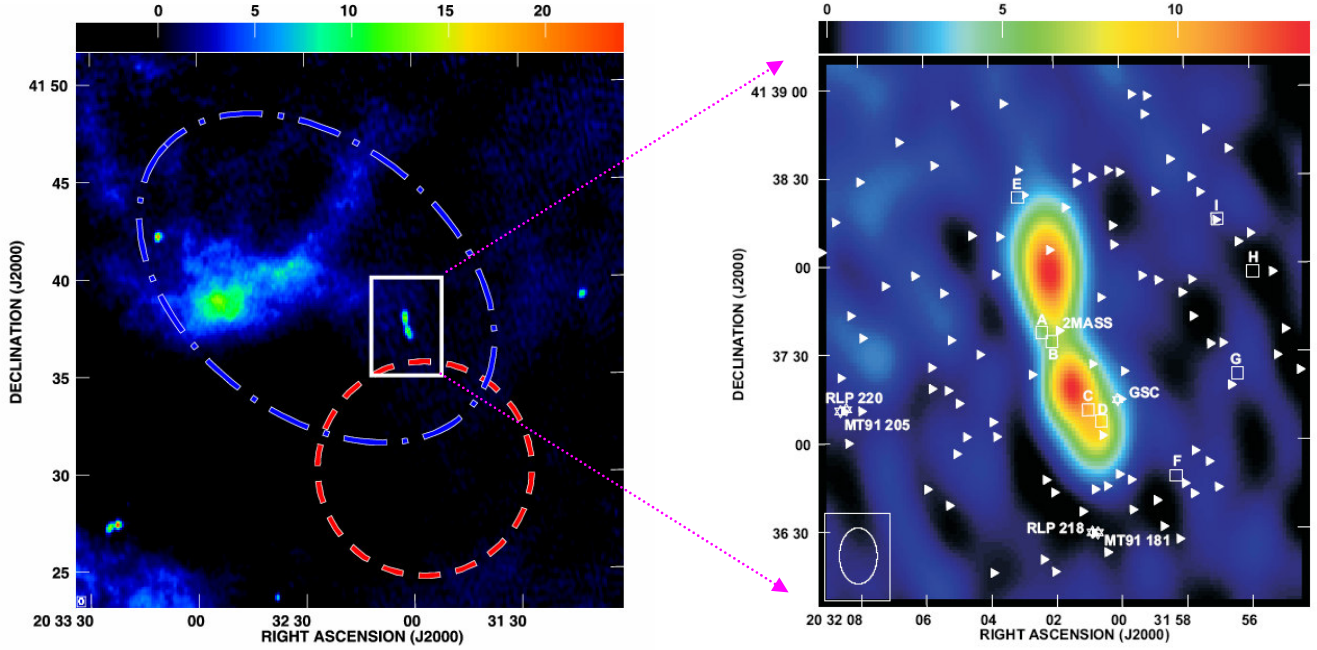


Figure 1: (left) 1400MHz WSRT map showing the *approximate* location of the Whipple TeV γ ray hotspot (blue) as well as the extended HEGRA emission region (red). Note that the Whipple hotspot does not necessarily correspond to an extended TeV gamma-ray emission region but is simply the highest likelihood region of γ ray emission, of either a point-like nature or an intrinsically extended region of radius less than ~ 7 arcmin. The blue ellipse shown corresponds roughly to the 600 excess counts level in Fig 3 of Konopelko et al. (2006). The other two non-thermal radio sources, WSRTGP 2031+4116 (also dual-lobed; $\alpha_{2000}, \delta_{2000} = 20\ 33\ 23.19\ +41\ 27\ 23.7$), and WSRTGP 2031+4131 ($\alpha_{2000}, \delta_{2000} = 20\ 33\ 10.6\ +41\ 42\ 11$) can be seen towards the lower-left and upper left regions of the figure, respectively. The large region of diffuse radio emission towards the center of the Whipple hotspot location is thermal in nature (see text). (right) A close-up of the dual-lobed non-thermal radio source of interest at 1.4GHz, overlaid w/ CHANDRA (\square) and 2MASS (\blacktriangleright) counterparts. CHANDRA sources have been labeled alphabetically. Stars are shown as (\star) and appear with their catalog names. GSC refers to the star GSC 03161-00887.

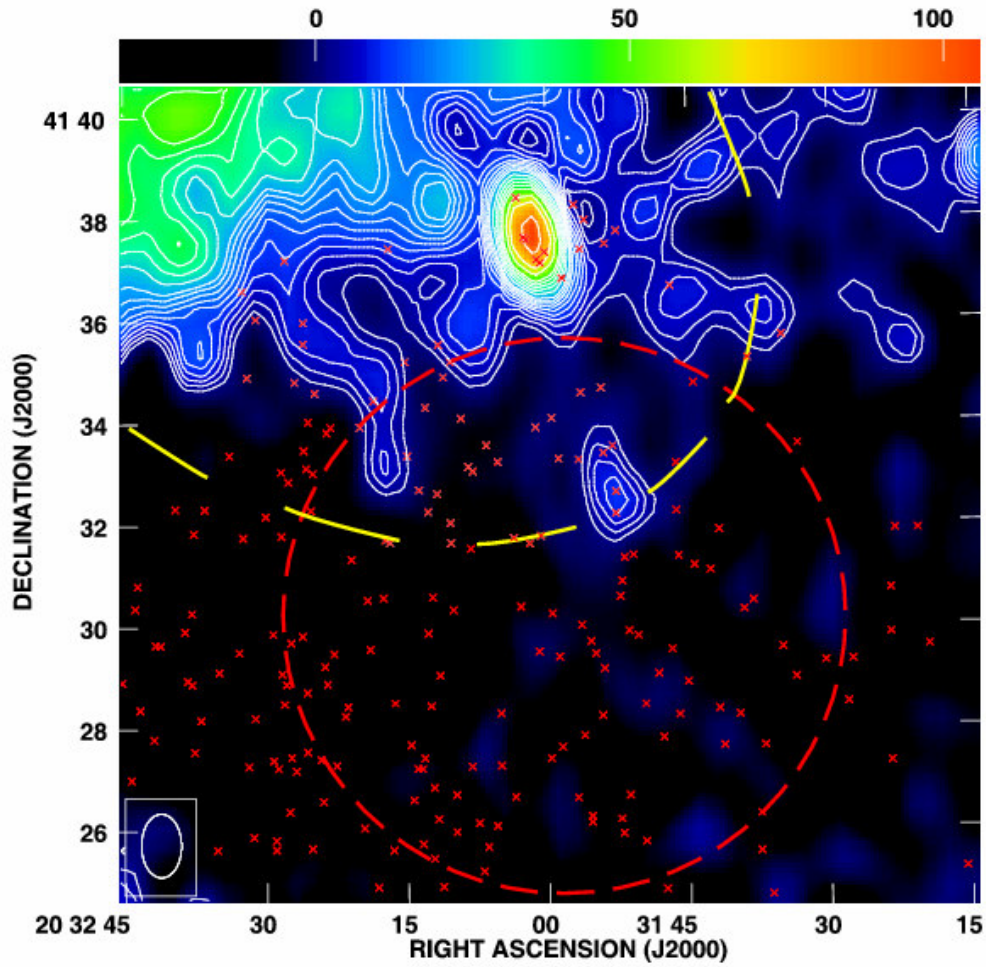


Figure 2: 365MHz WSRT data showing the diffuse non-thermal radio condensation at $\alpha_{2000}, \delta_{2000} = (20\ 31\ 53, +41\ 32\ 35)$ which is aligned with the radio-lobes and has a flux of ~ 11.6 mJy at 365 MHz. Since the resolution at 365 MHz is poorer than at 1400MHz the two lobes are not discernable in this image. CHANDRA X-ray sources are shown as red crosses, and the HEGRA (red) and Whipple (yellow) TeV emission regions are marked. Note that the CHANDRA field of view only covered part of the radio field displayed above.

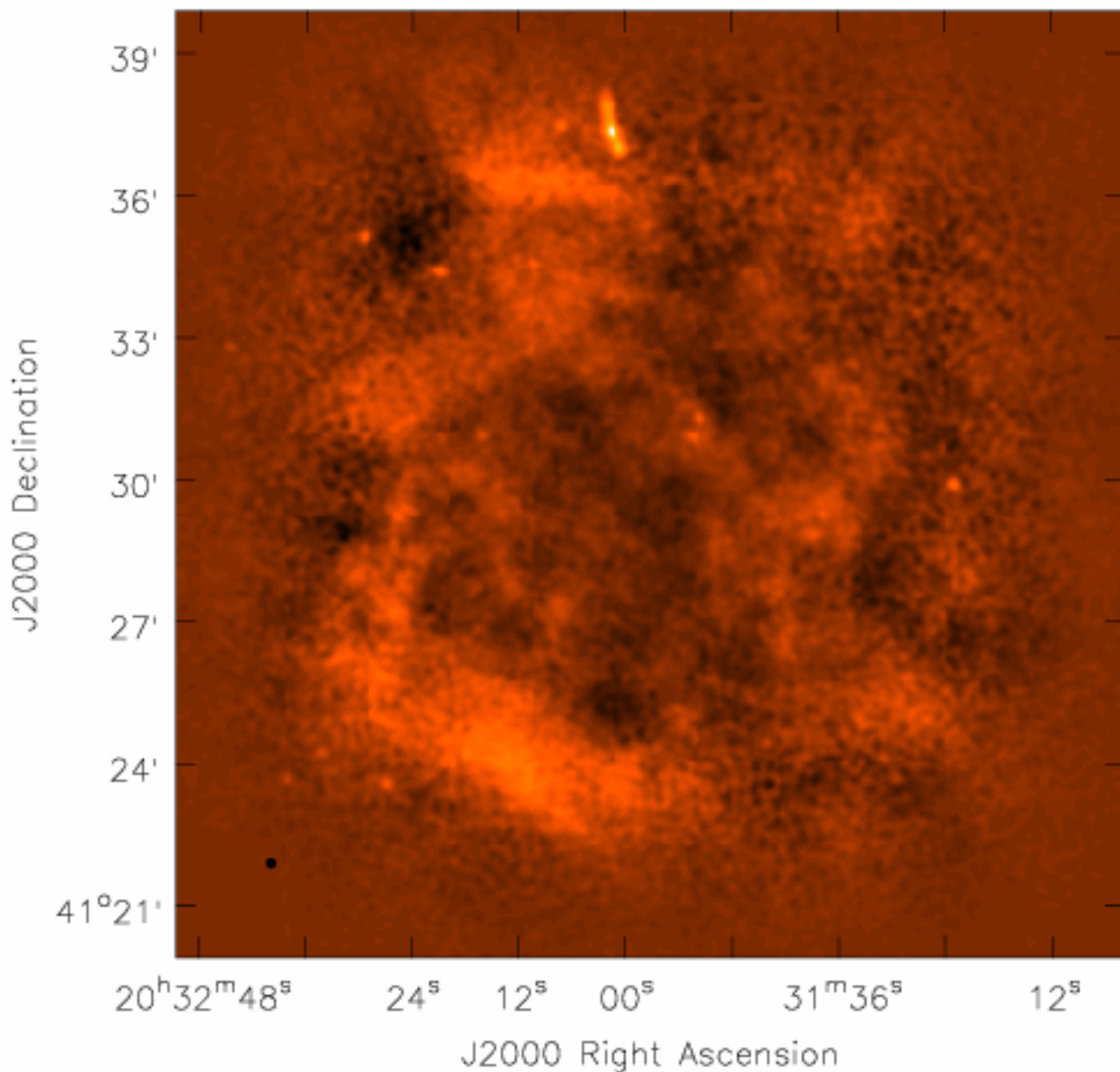


Figure 3: A mosaiced VLA image using 5 pointings at 4.8GHz taken 29 April 2003 (see text). The presence of weak ring-like structure(s) with center approximately $\alpha_{2000}, \delta_{2000} = (20\ 31\ 55, +41\ 29\ 00)$ and radius ~ 5 arcmin, consistent with the dimensions of the TeV source reported by HEGRA, is evident. The dual-lobed radio source can also be seen to the north. The spectral index of the ring varies, with the western side in general being more non-thermal, with $\alpha \sim -0.7$. As the eastern side is not detected at 1.4GHz (with an rms noise level of ~ 0.5 mJy/beam), that region is likely thermal with an index of about $\alpha \sim +0.6$, or larger. The flux density in the image ranges from -0.3 mJy/beam to 0.69 mJy/beam.